

# MASQUE: A Text-Guided Diffusion-Based Framework for Localized and Customized Adversarial Makeup

Youngjin Kwon  
CISPA Helmholtz Center for  
Information Security  
youngjin.kwon@cispa.de

Xiao Zhang  
CISPA Helmholtz Center for  
Information Security  
xiao.zhang@cispa.de

## Abstract

*As facial recognition is increasingly adopted for government and commercial services, its potential misuse has raised serious concerns about privacy and civil rights. To counteract, various anti-facial recognition techniques have been proposed for privacy protection by adversarially perturbing face images, among which generative makeup-based approaches are the most popular. However, these methods, designed primarily to impersonate specific target identities, can only achieve weak dodging success rates while increasing the risk of targeted abuse. In addition, they often introduce global visual artifacts or a lack of adaptability to accommodate diverse makeup prompts, compromising user satisfaction. To address the above limitations, we develop **MASQUE**, a novel diffusion-based framework that generates localized adversarial makeups guided by user-defined text prompts. Built upon precise null-text inversion, customized cross-attention fusion with masking, and a pairwise adversarial guidance mechanism using images of the same individual, **MASQUE** achieves robust dodging performance without requiring any external identity. Comprehensive evaluations on open-source facial recognition models and commercial APIs demonstrate that **MASQUE** significantly improves dodging success rates over all baselines, along with higher perceptual fidelity and stronger adaptability to various text makeup prompts.*

## 1. Introduction

Facial recognition (FR) systems [22] have been adopted in a wide range of security, biometrics, and commercial applications. However, their unregulated deployment poses serious privacy risks, allowing for unauthorized surveillance and malicious tracking. To address these concerns, *anti-facial recognition* (AFR) technologies [34] have emerged to protect user privacy from unauthorized FR systems. AFR techniques vary depending on which stage of facial recognition they disrupt and typically work by modifying images before they are

shared online. Among them, adversarial methods are particularly effective, subtly altering face images to evade detection while preserving their natural appearance. Traditional adversarial approaches, such as noise-based methods [13, 37, 41], obscure facial features with norm-bounded global perturbations, while patch-based techniques [15, 36] optimize adversarial patterns in localized image regions. However, these methods often introduce noticeable visual artifacts, compromising the usability of the produced images.

To overcome these limitations, recent work has shifted toward generative approaches, leveraging generative adversarial nets or diffusion models for AFR. Instead of relying on pixel-wise perturbations, these methods generate unrestricted yet semantically meaningful modifications that blend naturally into facial features. A notable direction is makeup-based AFR [7, 12, 26, 30, 38], which seamlessly integrates adversarial perturbations into makeup—a plausible approach, as makeup is inherently associated with facial appearance (see Appendix A for detailed discussions of related work).

While makeup-based AFR methods offer a promising balance between privacy protection and aesthetics, they often struggle to preserve fine-grained facial details or fully adhere to user instructions from diverse prompts. In addition, these methods require images of an external target identity to guide the generation process for adversarial makeup transfer and primarily focus on the impersonation setting for evaluation, increasing the risks of targeted abuse. When considering the more privacy-critical dodging scenarios, their performance in protection success rates also drops significantly.

**Contribution.** We propose **MASQUE**, a novel diffusion-based image editing method for localized adversarial makeup generation with customized text guidance. In particular, **MASQUE** is designed to meet the following desiderata simultaneously:

- *Inoffensive Identity Protection*: ensure high protection success rates in dodging scenarios without requiring images of a specific target identity.
- *Localized Modification*: restrict adversarial perturbations to designated areas, preserving all other facial details.

- *User Control*: demonstrate strong prompt-following ability and adaptability to diverse text makeup prompts.

## 2. Problem Formulation

In this section, we specify the threat model for unauthorized facial recognition (Section 2.1), introduce the background on anti-facial recognition (Section 2.2), and explain why dodging is more suitable than impersonation (Section 2.3).

### 2.1. Threat Model

We consider the adversarial setup, where an attacker adopts unauthorized FR models to identify benign users from their publicly shared facial images. This enables the extraction of sensitive information, posing significant privacy risks. Since many well-trained FR models are readily available—either as open-source implementations or through commercial APIs—attackers can easily obtain automated FR tools to achieve this malicious objective. Formally, let  $\mathcal{X}$  be the input facial image space and  $\mathcal{Y}$  be the set of possible identities. Given a collection of online-scraped face images  $\mathcal{D}$ , the adversary aims to correctly identify victim users from their facial images according to the following objective:

$$\max \sum_{(x,y) \in \mathcal{D}} \mathbb{1}(\text{FR}(x) = y), \quad (1)$$

where  $x$  stands for a face image,  $y$  is the corresponding ground-truth identity, and  $\text{FR} : \mathcal{X} \rightarrow \mathcal{Y}$  denotes a FR model.

A typical FR model consists of three key components: a feature extractor, a gallery database, and a query matching step (see [7, 34] for detailed descriptions). Aligned with prior work [26, 30], we assume that FR models employed by the attacker can achieve high accuracy on clean images. Since FR systems can vary in design, the attacker may utilize different feature extractors and query-matching schemes. To comprehensively assess performance under black-box conditions, we evaluate a range of well-trained FR models, from open-source models to commercial APIs. Additionally, we consider face verification as a specialized FR variant, where the gallery database contains only a single user.

### 2.2. Anti-Facial Recognition

The primary goal of AFR is to evade the identification of unauthorized facial recognition models used by adversaries described in Section 2.1, improving the protection of benign users’ privacy. In this work, we focus on the most popular adversarial-based AFR techniques, which craft imperceptible or naturalistic perturbations (e.g., adversarial makeup) to user’s images to fool FR systems. Specifically, the objective of *adversarial-based AFR* can be cast into a constrained

optimization problem as follows:

$$\begin{aligned} \max & \frac{1}{|\mathcal{D}|} \sum_{(x,y) \in \mathcal{D}} \mathbb{1}\{\text{FR}(\text{AFR}(x)) \neq y\} \\ \text{s.t.} & \frac{1}{|\mathcal{D}|} \sum_{(x,y) \in \mathcal{D}} \Delta(\text{AFR}(x), x) \leq \gamma, \end{aligned} \quad (2)$$

where  $\text{AFR} : \mathcal{X} \rightarrow \mathcal{X}$  denotes the AFR perturbation function,  $\Delta$  is a similarity metric that measures the visual distortion of the AFR-perturbed image  $\text{AFR}(x)$  with reference to the original image  $x$ , and  $\gamma > 0$  is a threshold parameter reflecting the distortion upper bound the user can tolerate.

**Dodging Success.** We consider benign users who seek privacy protection through adversarial-based AFR before sharing their facial images online. A desirable AFR technique should achieve a high *dodging success rate* (DSR) against unauthorized facial recognition, as defined by the optimization objective in Equation 2. For clarity, we refer to these users as *defenders*, as they apply AFR techniques to modify their facial images with adversarial perturbations. Since the defender typically lacks precise knowledge of the FR model employed by the attacker, we consider the black-box scenario when evaluating the DSR of each AFR method.

**Visual Quality.** From the user’s perspective, images perturbed by AFR should appear natural and closely resemble the original, as captured by the optimization constraint in Equation 2. If  $\text{AFR}(x)$  has an unsatisfactory image quality, users may be reluctant to share the protected face image online, even if a high DSR is achieved. Given this expectation of high visual quality, earlier privacy-preserving techniques such as face obfuscation or anonymization [20, 29] are not suitable. In comparison, makeup-based AFR methods [26, 30] stand out, as they introduce natural adversarial perturbations with minimal visual distortion. In this work, we further improve the performance of generative makeup-based AFR, enhancing both DSR and visual quality.

### 2.3. Why Dodging instead of Impersonation?

In contrast to the *untargeted* dodging objective, several state-of-the-art studies [12, 26, 30, 37] have focused on improving AFR performance in *targeted* impersonation scenarios. Impersonation-oriented methods aim to adversarially modify a user’s facial images to mislead a FR model into recognizing them as a specific target identity. Let  $\text{AFR}_I : \mathcal{X} \rightarrow \mathcal{X}$  be the perturbation function for an impersonation-oriented method. In existing literature, the *impersonation success rate* (ISR) is typically measured by the following metric:

$$\text{ISR} := \frac{1}{|\mathcal{D}|} \sum_{(x,y) \in \mathcal{D}} \mathbb{1}\{\text{FR}(\text{AFR}_I(x)) = y_t\}, \quad (3)$$

where  $y_t$  denotes the target identity satisfying  $y_t \neq y$ . Below, we further detail why impersonation is not suitable for AFR.

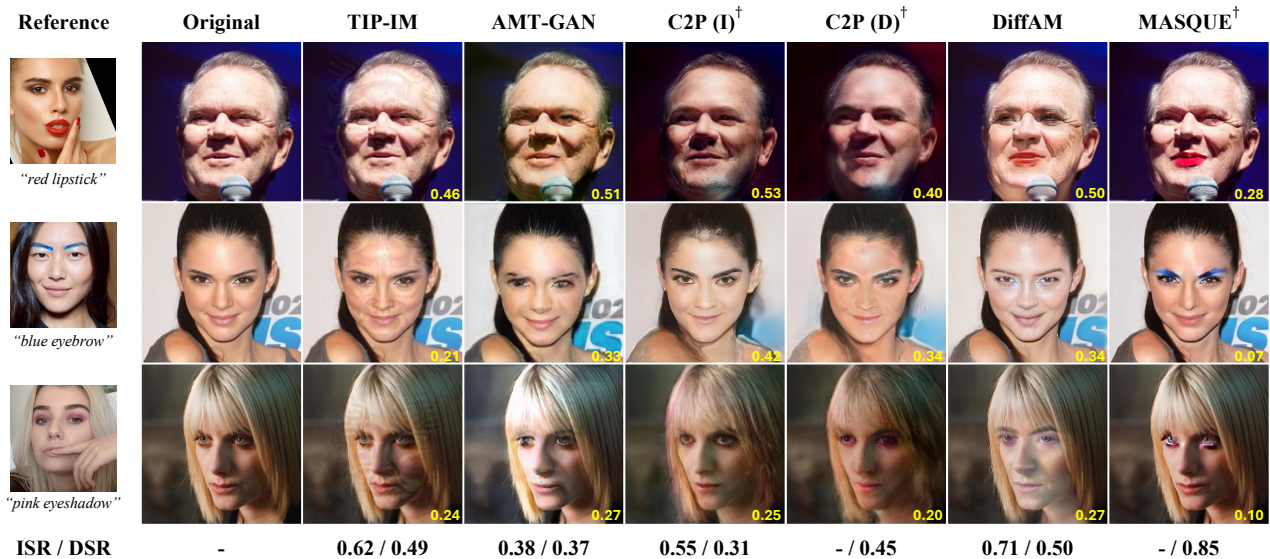


Figure 1. Each row presents the reference image with a text makeup prompt, the original image, followed by the generations of each AFR method. Methods marked with † require only a text prompt for makeup application and do not rely on a reference image. The yellow text indicates the cosine similarity score. Below the images, we compare ISR and DSR averaged across four FR models and three makeup styles.

**Misaligned Goal.** From the defender’s perspective, impersonation and dodging serve different goals, as reflected in their distinct evaluation metrics, ISR and DSR. As shown by [42], high ISR does not guarantee high DSR. If the target identity  $y_t$  is not included in the attacker’s model (e.g., using facial verification with only a single image of the victim identity  $y$ ), optimizing for higher ISR offers little benefit due to misaligned objectives. As we will illustrate in Section 3.1, prior impersonation-oriented AFR methods can only achieve weak privacy protection when evaluated under dodging scenarios. Therefore, we argue that effective privacy protection should prioritize *untargeted dodging success*.

**Targeted Misuse.** Impersonation increases the risk of targeted misuse, raising serious ethical and fairness concerns. Unlike dodging, impersonation-based approaches allow users to control the target identity they are mistaken for, making them more susceptible to abuse. This ability can be exploited for malicious purposes, such as falsely associating one’s actions with another individual. For instance, if a user  $y$  intentionally applies an AFR tool to impersonate a target  $y_t$  and engages in illegal activity, FR systems may misidentify  $y_t$  as the suspect. This deliberate identity manipulation poses significant ethical and legal risks [34].

By contrast, dodging-oriented AFR serves as a better solution for facial privacy protection. Instead of redirecting recognition to a specifically chosen identity, dodging causes misclassification in an uncontrolled manner, typically as an unknown or incorrect identity. This lack of control makes dodging significantly less susceptible to intentional misuse, as users cannot deliberately impersonate or frame a different

	Dodging	External ID	Guidance	Local	Prompt-Following
TIP-IM [37]	✗	✓	n/a	✗	n/a
AMT-GAN [12]	✗	✓	image	✗	low
C2P [26]	✓	✓	text	✗	medium
DiffAM [30]	✗	✓	image	✓	medium
MASQUE (ours)	✓	✗	text	✓	high

Table 1. Comparisons of SOTA AFR methods for key features in terms of both privacy protection and visual quality.

party. While dodging still prevents correct identification, it does so without assigning a specific false identity, reducing the risk of targeted deception or malicious intent.

### 3. Challenges of Existing AFR Methods

In this section, we present preliminary results to highlight key limitations of previous work, further motivating the design of our approach, which will be detailed in Section 4.

**Preliminary Results.** Figure 1 shows qualitative comparisons of three makeup styles, evaluating several prior AFR methods, including a noise-based method, TIP-IM [37], and three state-of-the-art makeup-based approaches [12, 26, 30]. For each AFR method, we report the metrics across different black-box facial verification models averaged across 100 randomly selected images from CelebA-HQ [14]. To ensure a fair comparison with image-guided AFR methods, we either select the corresponding makeup image from a benchmark facial makeup dataset [16] or generate one by inpainting the makeup on a non-makeup image (see Section 5.1 for more details). Table 1 summarizes the key feature comparisons of state-of-the-art AFR methods, including ours.

### 3.1. Weak Protection under Dodging

As discussed in Section 2.3, an ideal AFR should account for dodging scenarios, to ensure privacy without dependence on a target identity. However, despite its ethical advantages, dodging remains an underexplored and underdeveloped area in makeup-based AFR. Existing methods that perform well under impersonation settings often exhibit a significant drop in DSR, as shown in Figure 1. This highlights a fundamental gap: current techniques are not optimized for dodging, leaving privacy protection less reliable when a user seeks to avoid recognition rather than impersonate another identity. In addition, while some methods like [7, 26] introduce a form of dodging, they still rely on a target identity. This reliance contradicts the very goal of dodging-based AFR, which should function without any identity substitution. Thus, a key challenge in AFR research is developing a robust dodging-based approach that provides strong protection while avoiding the ethical risks associated with impersonation.

### 3.2. Non-Localized Face Modification

Noise-based approaches like TIP-IM generate global perturbations, which fail to localize the editings. Makeup-based AFR embeds perturbations within makeup to achieve a more natural disguise, but many GAN-based approaches, including AdvMakeup, AMT-GAN, and C2P, introduce global artifacts that alter non-facial regions. This lack of precise localization is particularly problematic when users seek to protect only their facial identity while preserving the background. As shown in Figure 1, this issue is especially pronounced in complex backgrounds, where perturbations should remain confined to facial regions but instead extend beyond. In contrast, the diffusion-based method DiffAM enables better localization, effectively applying makeup perturbations from a reference image. However, its reliance on reference images limits flexibility, particularly when suitable references are unavailable. This highlights the need for methods that achieve both precise localization and greater flexibility.

### 3.3. Limited Prompt-Following Ability

Makeup-based AFR methods aim to modify facial appearance to prevent accurate identification by FR systems. However, existing methods offer limited user control, making customization and usability a key challenge. Broadly, makeup-based AFR methods fall into two categories:

- *Image-reference-based AFR* transfers makeup styles from a reference image. While they aim for accurate replication, they struggle with reliability and flexibility. As shown in Figure 1, early GAN-based methods like AMT-GAN fail to transfer makeup consistently, while DiffAM, despite improvements, remains restricted. It only applies makeup to three fixed regions—skin, mouth, and eyes—preventing transfer to other areas like colored eyebrows. Additionally, these methods require separate fine-tuning for each

reference, limiting efficiency.

- *Text-prompt-based AFR* allows users to describe makeup styles in natural language, eliminating the need for reference images or separate fine-tuning while enhancing privacy. However, this method lacks fine-grained control, as C2P relies solely on CLIP directional loss, often leading to unintended modifications beyond the intended areas.

## 4. Our Methodology: MASQUE

To address the key challenges discussed in Section 3, we propose MASQUE, a method designed to disrupt FR models with localized adversarial makeup while ensuring no external identity is introduced. Figure 2 illustrates the pipeline of MASQUE with its pseudocode in Appendix D. The makeup is guided by a user-defined text prompt  $p^*$ , refined via cross-attention fusion with a mask. Pairwise adversarial guidance is further introduced to ensure these perturbations mislead FR systems without compromising visual fidelity.

Our method leverages the state-of-the-art Stable Diffusion [24] adapted to generate high-quality adversarial makeups by iterative denoising a random noise latent  $z_T$  conditioned on a text embedding  $C$ . To be more specific, Stable Diffusion is trained to predict the added noise  $\epsilon$  via:

$$\min_{\theta} \mathbb{E}_{z_0, \epsilon \sim \mathcal{N}(0, I), t \sim \text{Unif}(1, T)} \left[ \|\epsilon - \epsilon_{\theta}(z_t, t, C)\|_2^2 \right].$$

**Applying Makeup with Cross Attention.** Before applying edits, we first obtain a faithful latent representation of the original image  $x$  using *null-text inversion* [19], which mitigates reconstruction errors common in direct DDIM inversion [28]. Conditioning on an empty prompt to align the forward and reverse diffusion trajectories, ensuring near-perfect reconstruction of the image’s structure and identity.

With this accurate latent representation, we introduce makeup attributes via the text prompt  $p^*$  by manipulating the *cross-attention* (CA) layers of the diffusion model [24], which control how spatial features correspond to semantic tokens. At each diffusion step  $\tau$ , we extract attention maps  $A_{\tau}$  (reconstruction) and  $A_{\tau}^*$  (editing) and blend them: preserving CA values from  $A_{\tau}$  for shared tokens to maintain structure, while incorporating values from  $A_{\tau}^*$  for makeup-specific tokens in  $p^*$ :

$$\left(\text{Update}(A_{\tau}, A_{\tau}^*)\right)_{i,j} := \begin{cases} (A_{\tau})_{i,j}, & \text{if } j \text{ is in both } p \text{ and } p^*, \\ (A_{\tau}^*)_{i,j}, & \text{if } j \text{ is unique to } p^*, \end{cases}$$

where  $p$  denotes the original text prompt. The result is  $\hat{A}_{\tau}$ , a set of mixed CA maps that preserve the original facial layout while steadily introducing adversarial makeup features [9].

**Enhancing Semantic Edits and Locality.** To ensure precise localization, we generate a mask  $\mathcal{M}$  that defines the region

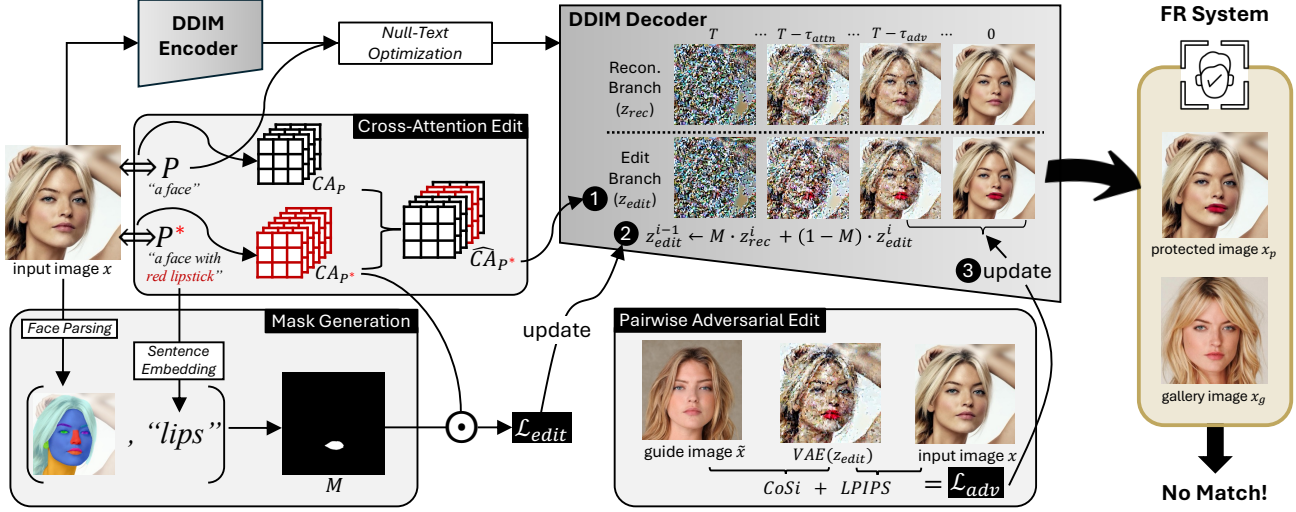


Figure 2. The pipeline of MASQUE involves: (1) fusing the editing and reconstruction prompts to produce an updated cross-attention map for diffusion, (2) creating a mask  $\mathcal{M}$  to define a target region and optimize an edit loss to maximize makeup-related attention in  $\mathcal{M}$ , and (3) using pairwise adversarial guidance with same-identity image to enhance identity confusion without external targets.

for modification. To achieve this, we embed the prompt  $p^*$  using a Sentence Transformer [23] model and compare it to embeddings of predefined facial regions. The closest match determines the relevant area for the edit. For instance, if the prompt specifies “a face with red lipstick”, the model identifies lips as the target and generates a lip-area mask. This ensures that our adversarial makeup perturbations remain focused on the correct facial region and do not unintentionally alter other parts of the face.

Once the target region  $\mathcal{M}$  is determined, we enhance the influence of makeup-related tokens by maximizing their attention within  $\mathcal{M}$ . This ensures that modifications are reinforced within the intended area, preventing unintended changes elsewhere and maintaining overall image quality [18]. Specifically, we optimize:

$$\mathcal{L}_{\text{edit}} = \left( 1 - \frac{1}{|\mathcal{M}|} \sum_{i \in \mathcal{M}} \frac{(A_{\tau}^*)_{i,\text{new}}}{(A_{\tau}^*)_{i,\text{new}} + \sum_{j \in \text{share}} (A_{\tau})_{i,j}} \right)^2,$$

where  $(A_{\tau}^*)_{i,\text{new}}$  is the attention weights assigned to the new makeup tokens at spatial index  $i$ , while  $\sum_{j \in \text{share}} (A_{\tau})_{i,j}$  is the total attention weight of tokens that appear in both the original and makeup prompts. By emphasizing makeup-specific attention in the masked region, this loss term ensures that modifications in  $x_p$  occur meaningfully in the intended region while preventing edits from spreading elsewhere.

To further enforce spatial precision, we process the latent through two distinct branches: an edit branch for makeup application and a reconstruction branch to preserve original features. During the backward steps, we explicitly constrain perturbations within the designated area by imposing the

following conditions:

$$z_{\text{edit}} = \mathcal{M} \cdot z_{\text{edit}} + (1 - \mathcal{M}) \cdot z_{\text{rec}},$$

where  $z_{\text{edit}}$  represents the latent from the edit branch, and  $z_{\text{rec}}$  denotes the latent from the reconstruction branch.

While makeup edits ensure semantic plausibility, the core adversarial objective is to disrupt FR models. Here lies our novel contribution: a *pairwise adversarial guidance* that uses a guide image of the same identity to achieve robust identity confusion without relying on an external target.

**Pairwise Adversarial Guidance.** Previous makeup-based AFR methods often target another identity, compromising privacy and limiting applicability in dodging scenarios. By contrast, our approach leverages a pair  $(x, \tilde{x})$  of face images from the same individual, where  $\tilde{x}$  serves as the guide image. This strategy highlights a significant issue with naively using the distance from the original image as the adversarial loss. Note that in the standard diffusion denoising process, the objective is to generate images similar to the original. If we merely maximize the distance from the original image as an adversarial loss, it can potentially create conflicting objectives, leading to an unstable performance in both image quality and adversarial effectiveness (see Tables 2-3 in Appendix B for supporting evidence and comparison results with self-augmented guide images).

**Adversarial and Image Quality Trade-off.** We introduce adversarial perturbations during the later stage of the diffusion process, ensuring coarse structure remains intact while subtly altering identity-specific features. To balance adversarial potency with visual fidelity, we incorporate perceptual similarity constraints alongside a *cosine similarity* (CoSi)

Method	CelebA-HQ				VGG-Face2-HQ				Avg.	
	IR152	IRSE50	FaceNet	MobileFace	IR152	IRSE50	FaceNet	MobileFace		
Identification	Clean	10.00	13.00	5.00	40.00	13.00	18.00	18.00	25.00	17.75
	TIP-IM	62.00	86.00	65.00	74.00	57.00	73.00	52.00	62.00	66.38
	AMT-GAN	61.22	48.33	50.67	57.33	16.00	24.00	22.33	32.33	39.03
	DiffAM	54.00	57.67	59.00	74.33	49.67	51.67	54.00	70.67	58.88
	C2P (I)	30.67	38.33	22.00	56.67	18.00	20.00	21.67	32.00	29.92
	C2P (D)	74.67	76.33	56.33	77.33	18.33	19.67	20.33	30.33	46.67
	MASQUE ( $G = 0$ )	92.33	95.67	61.33	87.00	69.67	76.33	45.33	81.67	76.17
	MASQUE ( $G = 1$ )	<u>98.00</u>	<u>98.33</u>	<u>77.67</u>	<u>94.00</u>	<u>84.33</u>	<u>89.00</u>	<u>61.00</u>	<u>91.00</u>	<u>85.50</u>
Verification	Clean	5.00	5.00	4.00	10.00	13.00	17.00	15.00	30.00	12.38
	TIP-IM	44.00	60.00	51.00	40.00	46.00	51.00	59.00	46.00	49.63
	AMT-GAN	40.00	32.00	51.67	25.67	14.00	26.33	26.67	40.67	32.13
	DiffAM	31.00	26.00	54.00	43.33	46.33	50.67	56.00	82.67	48.75
	C2P (I)	12.33	11.33	14.33	21.33	16.33	18.67	19.33	37.33	18.88
	C2P (D)	52.33	46.67	40.33	41.67	17.00	19.67	18.33	38.00	34.25
	MASQUE ( $G = 0$ )	89.33	90.67	57.67	76.33	62.33	71.33	42.33	86.00	72.00
	MASQUE ( $G = 1$ )	<u>96.00</u>	<u>96.67</u>	<u>75.67</u>	<u>79.33</u>	<u>82.33</u>	<u>91.67</u>	<u>63.33</u>	<u>94.33</u>	<u>84.92</u>

Table 2. Dodging success rate (%) under black-box facial identification and verification settings. For each column, the other three FR systems are used as surrogates to generate the protected faces, and the best result is underlined. Here,  $G$  denotes the number of guide images.

measure that captures adversarial effectiveness:

$$\mathcal{L}_{\text{adv}} = \lambda_{\text{CoSi}} \cdot \text{CoSi}(x_p, \tilde{x}) + \lambda_{\text{LPIPS}} \cdot \text{LPIPS}(x_p, x),$$

where  $x_p$  denotes the protected image. CoSi ensures that the adversarial perturbations sufficiently diverge from recognizable identity features, while LPIPS [39] maintains perceptual and structural fidelity, respectively. The parameters  $\lambda_{\text{CoSi}}$ ,  $\lambda_{\text{LPIPS}}$  allow fine-tuning of this trade-off. We conduct ablation studies to understand the sensitivity of these hyperparameters and how to set them in MASQUE for better trade-offs (see Section 5.3 and Appendix B).

## 5. Experiments

In this section, we conduct comprehensive experiments to study the effectiveness of MASQUE with comparisons to prior AFR methods in both privacy protection and visual aspects. Appendices B and C present additional experimental results and visualizations for more general makeup prompts.

### 5.1. Experimental Settings

**Dataset.** To reflect the high-quality nature of online facial images, we conduct experiments using 300 images from each of the CelebA-HQ [14] and VGG-Face2-HQ [3] datasets, all at a resolution of  $1024 \times 1024$ . We randomly sample 100 identities from per dataset, each with three images: a probe image to be protected, a reference image for guidance, and a the gallery image, which is assumed to be stored in the facial recognition system for comparison.

**Configuration.** We compare our methods against the following baselines: TIP-IM [37], the SOTA noised-based AFR,

and other recent generative-based AFR methods, including AMT-GAN [12], Clip2Protect [26], and DiffAM [30]. For Clip2Protect, we denote it as C2P for simplicity, where both the impersonating version (denoted as C2P (I)) and the dodging version (i.e., C2P (D)) are assessed. We compare the performance of MASQUE with existing AFR techniques on four public FR models: IR152 [6], IRSE50 [11], FaceNet [25], and MobileFace [2]. We also evaluate AFR methods against commercial FR APIs: Face++<sup>1</sup> and Luxand<sup>2</sup>.

For reference-based methods, we selected images from the makeup dataset [16] used during their pre-training, that best matched the given prompt. For the *blue eyebrow* style—introduced to assess performance on an uncommon makeup—finding a suitable reference was challenging, underscoring the limitations of reference-based methods for rare styles. To address this, we inpainted blue eyebrows on a non-makeup image from the dataset using our framework, excluding pairwise adversarial guidance, demonstrating its capacity for targeted edits without an external reference.

**Evaluation Metric.** We employ dodging success rate (DSR) as the primary evaluation metric for AFR. DSR is computed using a thresholding strategy for face verification and a closed-set strategy for face identification. For verification, specifically, DSR is defined as:

$$\text{DSR} = \frac{1}{N} \sum_x \mathbb{I}(\cos(\text{FR}(x_p), \text{FR}(x_g)) > \tau) \times 100\%,$$

where  $\mathbb{I}$  is the indicator function,  $N$  is the number of face images and FR represents the target face recognition model.

<sup>1</sup><https://www.faceplusplus.com/face-comparing/>

<sup>2</sup><https://luxand.cloud/face-api>

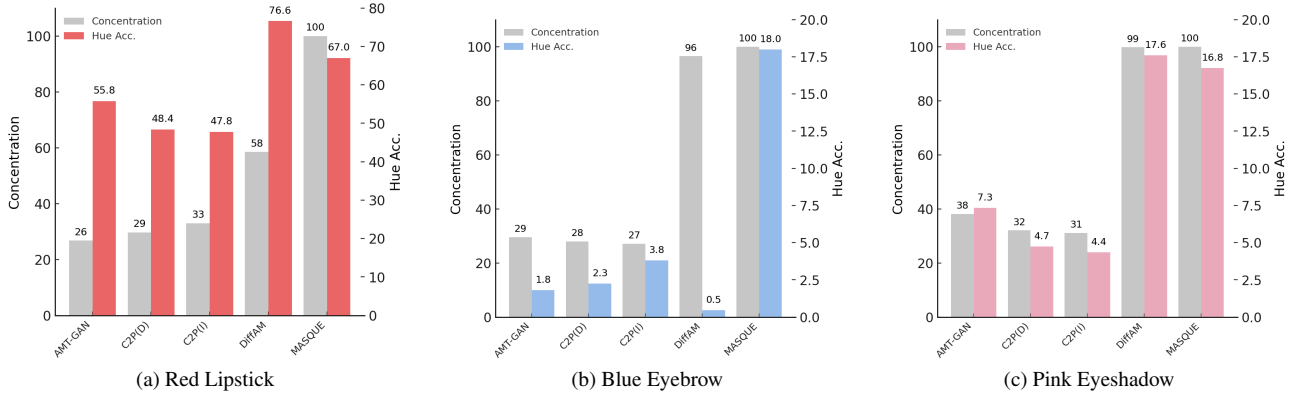


Figure 3. Comparison of concentration and hue accuracy across different methods for three makeup tasks: red lipstick, blue eyebrow, and pink eyeshadow. Concentration values are normalized relative to MASQUE.

$x_p$  denotes the protected image, while  $x_g$  stands for the gallery image of the corresponding identity. The similarity threshold  $\tau$  is set at a 0.01 *False Acceptance Rate* (FAR) for each victim model. For face identification, we use the *Rank-1 Accuracy*, which measures whether the top-1 candidate list excludes the original identity of  $x$ .

To assess the visual quality, we use LPIPS, PSNR, and SSIM [33]. A lower LPIPS score reflects higher perceptual similarity, while higher PSNR and SSIM values indicate better pixel-wise and structural fidelity to the original image.

**Implementation Detail.** MASQUE builds on the pre-trained Stable Diffusion v1.4 model, using DDIM denoising over  $T = 50$  steps with a fixed guidance scale of 7.5. During the backward diffusion process, CA injection occurs in  $[T, T - \tau_{\text{attn}}]$  ( $\tau_{\text{attn}} = 40$ ), localize optimization in  $[T, T - \tau_{\text{edit}}]$  ( $\tau_{\text{edit}} = 5$ ), and adversarial guidance in  $[T - \tau_{\text{adv}}, 0]$  ( $\tau_{\text{adv}} = 45$ ). We set  $\lambda_{\text{CoSi}} = 0.1$ ,  $\lambda_{\text{LPIPS}} = 1$ , and cap optimization to  $\text{max\_adv} = 15$  iterations.

## 5.2. Main Comparison Results

**Against Black-Box FR Models.** Table 2 presents the DSR for both face verification and Rank-1 identification in black-box scenarios, evaluated using four widely used pre-trained FR feature extractors [2, 6, 11, 25]. For each target model, the remaining three serve as surrogate models to simulate the black-box scenario, with results averaged across three makeup styles. Our method significantly outperforms all baselines, achieving an average DSR of 85.50% for identification and 84.92% for verification. In addition, while MASQUE without a guide image achieves a reasonable DSR, it still falls short compared to its guided counterpart. Furthermore, image quality degrades significantly without a guide image (see supporting evidence in Appendix B.2.).

**Real-world Performance.** We also test our method against the commercial APIs, Face++ and Luxand, in verification mode, which assigns similarity scores from 0 to 100. Figure

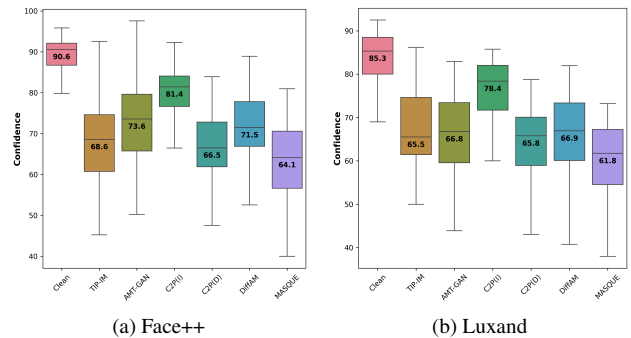


Figure 4. Performance comparisons against commercial FR APIs. Confidence scores (lower is better) from Face++ and Luxand show that MASQUE provides stronger privacy protection than state-of-the-art noise-based and makeup-based AFR approaches.

	TIP-IM	AMT-GAN	C2P(I)	C2P(D)	DiffAM	MASQUE
<b>LPIPS</b> (↓)	0.311	0.342	0.460	0.473	0.399	0.294
<b>PSNR</b> (↑)	32.158	19.512	18.922	17.990	18.314	25.815
<b>SSIM</b> (↑)	0.928	0.613	0.583	0.563	0.769	0.856

Table 3. Quantitative comparisons of the visual quality across different AFR methods. Lower values are better for LPIPS, while higher values are better for PSNR and SSIM.

4 shows the results. As a proprietary model with unknown training data and parameters, it serves as a realistic testbed for evaluating the effectiveness of AFR methods. Our approach achieves the lowest similarity score across both APIs, demonstrating effectiveness in both open-source and closed-source settings, reinforcing its real-world applicability.

**Visual Quality.** Our method achieves superior image quality across multiple evaluation metrics, as summarized in Table 3 and illustrated in Figure 1. While TIP-IM attains the highest PSNR and SSIM due to its small perturbation budget, these pixel-level metrics often fail to reflect perceptual quality. In contrast, our approach prioritizes perceptual consistency, balancing content fidelity and visual realism, as demonstrated

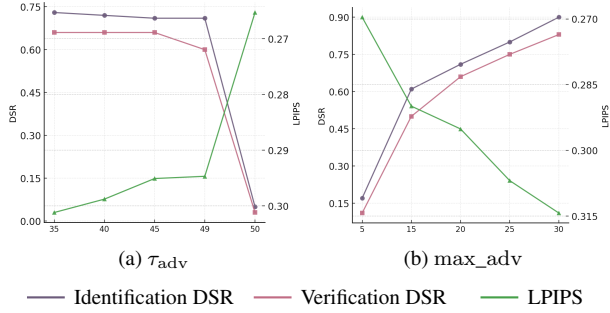


Figure 5. Ablation studies on hyperparameters  $\tau_{adv}$  and  $max\_adv$ , highlighting the trade-off between DSR and image quality.

by its strong LPIPS performance. We also confirm the advantages of MASQUE over existing AFR methods in achieving precise, localized makeup transfer (see additional experiments in Appendix B.1).

**Prompt Adherence.** We assess prompt adherence in terms of spatial precision and color accuracy. For spatial adherence, we use *Concentration*, which quantifies the proportion of modifications within a binary mask of the target area. Higher scores indicate better localization, while lower scores suggest spillover. For color precision, we evaluate *Hue Accuracy* by extracting modified pixels within the mask, converting them to HSV space, and measuring how many fall within the expected hue range. Figure 3 shows that MASQUE consistently achieves the highest concentration scores and competitive hue accuracy across prompts, ensuring precise localization with accurate color application. In contrast, DiffAM struggles with blue eyebrows, likely due to its framework restricting makeup transfer to specific facial regions, limiting its flexibility. These results confirm that MASQUE achieves strong prompt adherence by maintaining spatial precision while accurately reflecting the intended color attributes.

### 5.3. Ablation Studies

**Adversarial Strength vs. Image Quality.** Increasing  $\tau_{adv}$  enhances the adversarial effect, improving DSR but degrading image quality, as indicated by higher LPIPS values in Figure 5. Similarly, increasing  $max\_adv$  amplifies protection but further compromises image quality.

**Customized Makeup.** Figure 6 demonstrates the controllability of MASQUE across the following three distinct aspects. Additional visualizations are available in the Appendix C.

*Sequential Editing.* MASQUE enables progressive makeup application, allowing users to apply makeup sequentially to multiple facial areas. Each additional layer of makeup enhances the protection effect, as reflected in the decreasing similarity scores shown in Figure 6.

*Intensity Control.* The intensity of the makeup can be adjusted via text prompts. A simple modifier like “vivid” alters

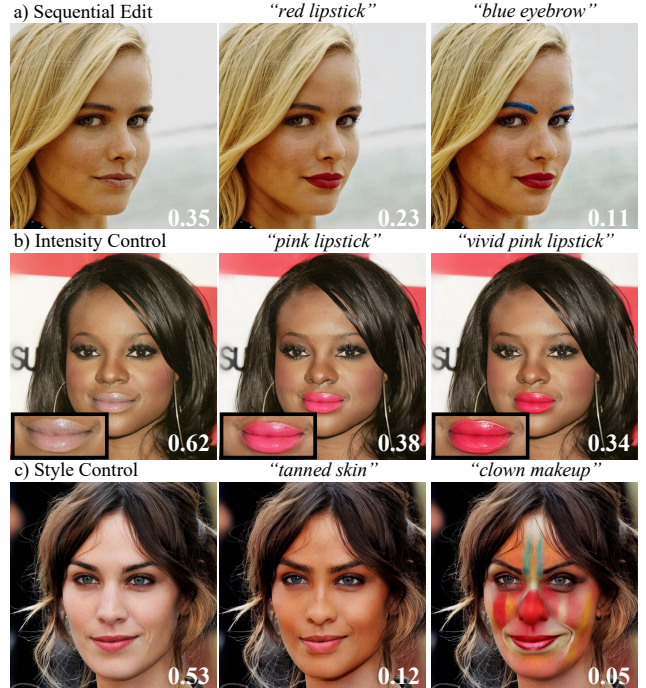


Figure 6. Examples showing the controllability of MASQUE through text prompts. The number at the bottom right indicates the similarity score between the image and the corresponding gallery image.

the cross-attention, resulting in color changes. Intensity variation has minimal effect on adversarial effectiveness.

*Style Control.* MASQUE supports full-face transformations. Prompts like “tanned skin” can blend naturally, while dramatic styles like “clown makeup” are also well-adapted. Greater makeup coverage further strengthens protection.

## 6. Further Discussions

**Guide Images.** While MASQUE with guide images enhance DSR and image quality, they may not always be available. As an alternative, we test self-augmented inputs as guide images via flipping and translation. However, preliminary results in Appendix B show limited improvements, indicating the need for more effective strategies to substitute the guide image.

**Computational Efficiency.** MASQUE enables adversarial makeup applications without pretraining. However, due to the iterative nature of diffusion models, inference speed remains a computational bottleneck. Future work can explore acceleration schemes to improve the efficiency of MASQUE.

**Adaptive Evaluations.** Real-world AFR threats evolve, with attackers refining strategies over time [7]. Considering adaptive scenarios, such as post-processing transformations (e.g., compression, smoothing, and makeup removal) and adversarial fine-tuning, could help improve robustness and provide a more comprehensive evaluation of AFR methods.



## 7. Conclusion

We introduced **MASQUE**, a diffusion-based AFR framework that applies adversarial makeup via text prompts, enabling localized modifications with automatically generated masks. Unlike prior AFR methods, **MASQUE** achieves high DSR while preserving visual quality without relying on external IDs, mitigating the potential risks of targeted misuse. Our experiments demonstrated the strong performance of **MASQUE**, where we highlight the important role of pairwise adversarial guidance. Future work may focus on real-time optimization and robustness against evolving FR models to further strengthen facial privacy protection.

## Availability

The code implementation of **MASQUE** and our experiments are open-sourced and available at <https://github.com/TrustMLRG/MASQUE>.

## References

- [1] Omri Avrahami, Ohad Fried, and Dani Lischinski. Blended latent diffusion. *ACM transactions on graphics (TOG)*, 42(4): 1–11, 2023. 11
- [2] Sheng Chen, Yang Liu, Xiang Gao, and Zhen Han. Mobilefacenets: Efficient cnns for accurate real-time face verification on mobile devices. In *Biometric Recognition: 13th Chinese Conference, CCBR 2018, Urumqi, China, August 11-12, 2018, Proceedings 13*, pages 428–438. Springer, 2018. 6, 7
- [3] Xuanhong Chen, Bingbing Ni, Yutian Liu, Naiyuan Liu, Zhilin Zeng, and Hang Wang. Simswap++: Towards faster and high-quality identity swapping. *IEEE Trans. Pattern Anal. Mach. Intell.*, 46(1):576–592, 2024. 6
- [4] Valeriia Cherepanova, Micah Goldblum, Harrison Foley, Shiyuan Duan, John Dickerson, Gavin Taylor, and Tom Goldstein. Lowkey: Leveraging adversarial attacks to protect social media users from facial recognition. *arXiv preprint arXiv:2101.07922*, 2021. 11
- [5] Guillaume Couairon, Jakob Verbeek, Holger Schwenk, and Matthieu Cord. Diffedit: Diffusion-based semantic image editing with mask guidance. *arXiv preprint arXiv:2210.11427*, 2022. 11
- [6] Jiankang Deng, Jia Guo, Niannan Xue, and Stefanos Zafeiriou. Arcface: Additive angular margin loss for deep face recognition. In *Proceedings of the IEEE/CVF conference on computer vision and pattern recognition*, pages 4690–4699, 2019. 6, 7
- [7] Wenshu Fan, Mingxing Zhang, Hongwei Li, Wenbo Jiang, Hanxiao Chen, Xiangyu Yue, Michael Backes, and Xiao Zhang. Divtrackee versus dyntacker: Promoting diversity in anti-facial recognition against dynamic fr strategy. *arXiv preprint arXiv:2501.06533*, 2025. 1, 2, 4, 8
- [8] Ian Goodfellow, Jean Pouget-Abadie, Mehdi Mirza, Bing Xu, David Warde-Farley, Sherjil Ozair, Aaron Courville, and Yoshua Bengio. Generative adversarial nets. *Advances in neural information processing systems*, 27, 2014. 11
- [9] Amir Hertz, Ron Mokady, Jay Tenenbaum, Kfir Aberman, Yael Pritch, and Daniel Cohen-Or. Prompt-to-prompt image editing with cross attention control. *arXiv preprint arXiv:2208.01626*, 2022. 4, 11
- [10] Jonathan Ho, Ajay Jain, and Pieter Abbeel. Denoising diffusion probabilistic models. *Advances in neural information processing systems*, 33:6840–6851, 2020. 11
- [11] Jie Hu, Li Shen, and Gang Sun. Squeeze-and-excitation networks. In *Proceedings of the IEEE conference on computer vision and pattern recognition*, pages 7132–7141, 2018. 6, 7
- [12] Shengshan Hu, Xiaogeng Liu, Yechao Zhang, Minghui Li, Leo Yu Zhang, Hai Jin, and Libing Wu. Protecting facial privacy: Generating adversarial identity masks via style-robust makeup transfer. In *Proceedings of the IEEE/CVF Conference on Computer Vision and Pattern Recognition*, pages 15014–15023, 2022. 1, 2, 3, 6, 11
- [13] Seong Joon Oh, Mario Fritz, and Bernt Schiele. Adversarial image perturbation for privacy protection—a game theory perspective. In *Proceedings of the IEEE International Conference on Computer Vision*, pages 1482–1491, 2017. 1
- [14] Tero Karras, Timo Aila, Samuli Laine, and Jaakko Lehtinen. Progressive growing of gans for improved quality, stability, and variation. *arXiv preprint arXiv:1710.10196*, 2017. 3, 6
- [15] Stepan Komkov and Aleksandr Petiushko. Advhat: Real-world adversarial attack on arcface face id system. In *2020 25th international conference on pattern recognition (ICPR)*, pages 819–826. IEEE, 2021. 1
- [16] Tingting Li, Ruihe Qian, Chao Dong, Si Liu, Qiong Yan, Wenwu Zhu, and Liang Lin. Beautygan: Instance-level facial makeup transfer with deep generative adversarial network. In *Proceedings of the 26th ACM international conference on Multimedia*, pages 645–653, 2018. 3, 6, 11
- [17] Qingjie Liu, Huanyu Zhou, Qizhi Xu, Xiangyu Liu, and Yunhong Wang. Psgan: A generative adversarial network for remote sensing image pan-sharpening. *IEEE Transactions on Geoscience and Remote Sensing*, 59(12):10227–10242, 2020. 11
- [18] Qi Mao, Lan Chen, Yuchao Gu, Zhen Fang, and Mike Zheng Shou. Mag-edit: Localized image editing in complex scenarios via mask-based attention-adjusted guidance. *arXiv preprint arXiv:2312.11396*, 2023. 5, 11
- [19] Ron Mokady, Amir Hertz, Kfir Aberman, Yael Pritch, and Daniel Cohen-Or. Null-text inversion for editing real images using guided diffusion models. In *Proceedings of the IEEE/CVF Conference on Computer Vision and Pattern Recognition*, pages 6038–6047, 2023. 4
- [20] Elaine M Newton, Latanya Sweeney, and Bradley Malin. Preserving privacy by de-identifying face images. *IEEE transactions on Knowledge and Data Engineering*, 17(2):232–243, 2005. 2, 11
- [21] Thao Nguyen, Anh Tuan Tran, and Minh Hoai. Lipstick ain’t enough: beyond color matching for in-the-wild makeup transfer. In *Proceedings of the IEEE/CVF Conference on computer vision and pattern recognition*, pages 13305–13314, 2021. 11
- [22] Omkar Parkhi, Andrea Vedaldi, and Andrew Zisserman. Deep face recognition. In *BMVC 2015-Proceedings of the British*

- Machine Vision Conference 2015*. British Machine Vision Association, 2015. [1](#)
- [23] Nils Reimers and Iryna Gurevych. Sentence-bert: Sentence embeddings using siamese bert-networks. In *Proceedings of the 2019 Conference on Empirical Methods in Natural Language Processing*. Association for Computational Linguistics, 2019. [5](#)
- [24] Robin Rombach, Andreas Blattmann, Dominik Lorenz, Patrick Esser, and Björn Ommer. High-resolution image synthesis with latent diffusion models. In *Proceedings of the IEEE/CVF conference on computer vision and pattern recognition*, pages 10684–10695, 2022. [4](#)
- [25] Florian Schroff, Dmitry Kalenichenko, and James Philbin. Facenet: A unified embedding for face recognition and clustering. In *Proceedings of the IEEE conference on computer vision and pattern recognition*, pages 815–823, 2015. [6](#), [7](#)
- [26] Fahad Shamshad, Muzammal Naseer, and Karthik Nandakumar. Clip2protect: Protecting facial privacy using text-guided makeup via adversarial latent search. In *Proceedings of the IEEE/CVF Conference on Computer Vision and Pattern Recognition*, pages 20595–20605, 2023. [1](#), [2](#), [3](#), [4](#), [6](#), [11](#)
- [27] Shawn Shan, Emily Wenger, Jiayun Zhang, Huiying Li, Haitao Zheng, and Ben Y Zhao. Fawkes: Protecting privacy against unauthorized deep learning models. In *29th USENIX security symposium (USENIX Security 20)*, pages 1589–1604, 2020. [11](#)
- [28] Jiaming Song, Chenlin Meng, and Stefano Ermon. Denoising diffusion implicit models. *arXiv preprint arXiv:2010.02502*, 2020. [4](#)
- [29] Qianru Sun, Liqian Ma, Seong Joon Oh, Luc Van Gool, Bernt Schiele, and Mario Fritz. Natural and effective obfuscation by head inpainting. In *Proceedings of the IEEE conference on computer vision and pattern recognition*, pages 5050–5059, 2018. [2](#)
- [30] Yuhao Sun, Lingyun Yu, Hongtao Xie, Jiaming Li, and Yongdong Zhang. Diffam: Diffusion-based adversarial makeup transfer for facial privacy protection. In *Proceedings of the IEEE/CVF Conference on Computer Vision and Pattern Recognition*, pages 24584–24594, 2024. [1](#), [2](#), [3](#), [6](#), [11](#)
- [31] Zhaoyang Sun, Shengwu Xiong, Yaxiong Chen, Fei Du, Weihua Chen, Fan Wang, and Yi Rong. Shmt: Self-supervised hierarchical makeup transfer via latent diffusion models. *arXiv preprint arXiv:2412.11058*, 2024. [11](#)
- [32] Narek Tumanyan, Michal Geyer, Shai Bagon, and Tali Dekel. Plug-and-play diffusion features for text-driven image-to-image translation. In *Proceedings of the IEEE/CVF Conference on Computer Vision and Pattern Recognition*, pages 1921–1930, 2023. [11](#)
- [33] Zhou Wang, Alan C Bovik, Hamid R Sheikh, and Eero P Simoncelli. Image quality assessment: from error visibility to structural similarity. *IEEE transactions on image processing*, 13(4):600–612, 2004. [7](#)
- [34] Emily Wenger, Shawn Shan, Haitao Zheng, and Ben Y Zhao. Sok: Anti-facial recognition technology. In *2023 IEEE Symposium on Security and Privacy (SP)*, pages 864–881. IEEE, 2023. [1](#), [2](#), [3](#)
- [35] Jianfeng Xiang, Junliang Chen, Wenshuang Liu, Xianxu Hou, and Linlin Shen. Ramgan: region attentive morphing gan for region-level makeup transfer. In *European Conference on Computer Vision*, pages 719–735. Springer, 2022. [11](#)
- [36] Zihao Xiao, Xianfeng Gao, Chilin Fu, Yinpeng Dong, Wei Gao, Xiaolu Zhang, Jun Zhou, and Jun Zhu. Improving transferability of adversarial patches on face recognition with generative models. In *Proceedings of the IEEE/CVF conference on computer vision and pattern recognition*, pages 11845–11854, 2021. [1](#)
- [37] Xiao Yang, Yinpeng Dong, Tianyu Pang, Hang Su, Jun Zhu, Yuefeng Chen, and Hui Xue. Towards face encryption by generating adversarial identity masks. In *Proceedings of the IEEE/CVF International Conference on Computer Vision*, pages 3897–3907, 2021. [1](#), [2](#), [3](#), [6](#), [11](#), [12](#)
- [38] Bangjie Yin, Wenxuan Wang, Taiping Yao, Junfeng Guo, Zelun Kong, Shouhong Ding, Jilin Li, and Cong Liu. Advmakeup: A new imperceptible and transferable attack on face recognition. *arXiv preprint arXiv:2105.03162*, 2021. [1](#), [11](#)
- [39] Richard Zhang, Phillip Isola, Alexei A Efros, Eli Shechtman, and Oliver Wang. The unreasonable effectiveness of deep features as a perceptual metric. In *Proceedings of the IEEE conference on computer vision and pattern recognition*, pages 586–595, 2018. [6](#)
- [40] Yuxuan Zhang, Lifu Wei, Qing Zhang, Yiren Song, Jiaming Liu, Huaxia Li, Xu Tang, Yao Hu, and Haibo Zhao. Stablemakeup: When real-world makeup transfer meets diffusion model. *arXiv preprint arXiv:2403.07764*, 2024. [11](#)
- [41] Yaoyao Zhong and Weihong Deng. Opom: Customized invisible cloak towards face privacy protection. *IEEE Transactions on Pattern Analysis and Machine Intelligence*, 45(3):3590–3603, 2022. [1](#)
- [42] Fengfan Zhou, Qianyu Zhou, Bangjie Yin, Hui Zheng, Xuequan Lu, Lizhuang Ma, and Hefei Ling. Rethinking impersonation and dodging attacks on face recognition systems. In *Proceedings of the 32nd ACM International Conference on Multimedia*, pages 2487–2496, 2024. [3](#)

## A. Related Work

### A.1. Anti-Facial Recognition

Earlier works on AFR proposed to use obfuscation techniques to obscure the facial identity features [20] or craft  $\ell_p$ -norm bounded perturbations to fool FR models [37]. While effective, these methods often compromise image quality, limiting their practicality in real-world scenarios. Poisoning-based methods [4, 27] introduced a new approach by injecting subtle adversarial noise into images to degrade the effectiveness of recognition models. These techniques excel at disrupting model training or inference without visibly altering the image, but their reliance on model-specific perturbations limits their generalizability across diverse architectures. Unrestricted adversarial examples, which aim to create natural-looking modifications, marked a significant advancement by integrating adversarial signals into realistic alterations without relying on specific constraints. These strategies leverage the flexibility of generative models to balance visual coherence and adversarial effectiveness.

**Adversarial Makeup.** Adversarial makeup [12, 26, 30, 38] has emerged as a practical solution to realize the goal of facial privacy protection. These methods leverage the strong generative capability of generative models to embed adversarial perturbations into natural makeup-based facial modifications, deceiving attackers’ facial recognition models while largely preserving the aesthetic appeal. For example, [12] proposed AMT-GAN, which introduces a regularization module and a joint training pipeline for adversarial makeup transfer within the generative adversarial network (GAN) framework [8]. Recent advancements in generative models have enhanced the performance of adversarial makeup transfer, such as Clip2Protect [26] and DiffAM [30], which adopt text-guided StyleGAN model and diffusion-based framework, respectively, to enable seamless adversarial face modifications with much improved visual quality. In this work, we build upon these developments by leveraging diffusion models to generate visually consistent, localized adversarial makeup for privacy protection in dodging scenarios.

### A.2. Diffusion-Based Image Editing

**Localized Image Editing.** Localized editing methods extend diffusion models for targeted modifications. For example, mask-based approaches [1, 5] constrain edits to specific regions using spatial masks, preserving unedited areas but often struggling with structural consistency. Attention-based approaches [9, 32] guide edits via attention injection, achieving better global structure preservation but suffering from unintended changes (editing leakage). Our proposed method, MASQUE, utilizes both mask-based and attention-based guidance without any fine-tuning, combining mask precision with attention flexibility, ensuring semantically consistent and region-specific modifications while addressing the limi-

tations of prior approaches.

**Text-Guided Diffusion Models.** Text-guided diffusion models are a major advancement in generative AI, capable of synthesizing high-quality images from natural language descriptions. Built on denoising diffusion probabilistic models (DDPMs) [10], they iteratively refine random noise into coherent images guided by text prompts. Recent advancements in diffusion models have expanded their capabilities to tasks such as localized editing and controllable generation. Mask-based approaches [1, 5?] achieve local text-guided modifications by incorporating user-defined constraints, like masks, to confine edits to specific regions. While effective in preserving unedited areas, these methods often struggle to maintain structural consistency within the edited regions, especially in complex scenarios. On the other hand, mask-free attention-based methods [9, 32?] use attention injection mechanisms to guide edits without requiring explicit masks. These methods excel at preserving the global structure of the image but are prone to editing leakage, where changes unintentionally affect areas beyond the intended region. In this work, we leverage mask-based cross-attention guidance [18] to achieve localized adversarial perturbations in the form of makeup. This approach ensures the precise application of modifications to desired regions, guided by user-specified prompts while addressing the limitations of structural inconsistencies seen in previous methods.

### A.3. Makeup Transfer

Advancements in makeup transfer have moved from GAN-based methods to more advanced diffusion models. Traditional approaches like BeautyGAN [16] and PSGAN [17] use histogram matching, attention mechanisms, and spatial encodings to transfer makeup while preserving structure. CPM [21] expands beyond color transfer using UV mapping, while RamGAN [35] ensure component consistency. However, GAN-based models struggle with extreme styles and rely on imprecise pseudo-paired data, limiting fidelity.

To overcome these challenges, diffusion-based methods like SHMT [31] and Stable-Makeup [40] offer improved realism and robustness. Specifically, SHMT eliminates reliance on pseudo-paired data through a self-supervised “decoupling-and-reconstruction” framework, leveraging a Laplacian pyramid for hierarchical texture transfer. Stable-Makeup employs a diffusion model with a Detail-Preserving encoder and cross-attention layers to ensure precise, structure-preserving makeup application. These approaches set a new standard for high-fidelity transfer. However, our study takes a different approach—rather than transferring makeup from a reference image, we focus on text-guided makeup generation using diffusion models, enabling intuitive and flexible image editing to create customizable makeup based solely on textual descriptions. This also eliminates the need for model fine-tuning on specific makeup images, allowing us

Metric	Method	In-Mask	Out-Mask	Diff $\Delta$
DISTS ( $\downarrow$ )	TIP-IM	2.013	0.094	1.919
	AMT-GAN	7.993	0.149	7.844
	C2P (I)	8.945	0.153	8.792
	C2P (D)	10.011	0.169	9.842
	DiffAM	9.645	0.141	9.504
	MASQUE	12.306	0.104	12.202
LPIPS ( $\downarrow$ )	TIP-IM	0.322	0.305	0.017
	AMT-GAN	0.360	0.316	0.044
	C2P (I)	0.400	0.447	-0.047
	C2P (D)	0.436	0.460	-0.025
	DiffAM	0.509	0.410	0.099
	MASQUE	0.434	0.290	0.144
PieAPP ( $\downarrow$ )	TIP-IM	3.621	0.462	3.1591
	AMT-GAN	21.325	0.814	20.511
	C2P (I)	17.186	1.138	16.049
	C2P (D)	20.850	1.314	19.536
	DiffAM	17.523	1.312	16.211
	MASQUE	21.433	0.645	20.789

Table 4. Comparison of perceptual similarity metrics across in-mask and out-mask regions and different AFR methods.

to generate the desired makeup directly during inference, resulting in a more efficient and adaptable approach.

## B. Additional Experiments

### B.1. Localized Editing

To evaluate whether edits are confined to the desired region, images are divided into in-mask and out-mask regions using a binary mask, isolating the corresponding areas in both images via element-wise multiplication. The areas are then used to normalize similarity metrics proportionally, ensuring fair comparisons. Specifically, we employ DISTS, LPIPS, and PieAPP as evaluation metrics in this experiment: DISTS measures perceptual dissimilarity based on structure and texture, LPIPS uses deep features, and PieAPP reflects human perceptual preferences.

Table 4 compares the effectiveness of localized edits, where higher  $\Delta$  values indicate stronger localization of perturbations. TIP-IM [37], as a noise-based method, applies pixel-wise adversarial perturbations uniformly, resulting in the smallest difference for all metrics due to minimal distinction between in-mask and out-mask regions. In contrast, our method introduces significant perturbations in the in-mask region, leading to poorer metrics there, but achieves the best or second-best results in the out-mask region, indicating minimal disruption to untouched areas.

### B.2. Pairwise Adversarial Guidance

MASQUE introduces pairwise adversarial guidance to protect identities without external target references, distinguishing it from impersonation-oriented methods. By aligning features between the guide and original images, we identify

#Guide	Iden. DSR( $\uparrow$ )	Veri. DSR( $\uparrow$ )	Confidence( $\uparrow$ )	Similarity( $\downarrow$ )	LPIPS( $\downarrow$ )
0	0.66	0.60	0.114	0.355	0.303
1	0.67	0.63	0.135	0.349	0.292
2	0.72	0.71	0.165	0.297	0.291
5	0.74	0.74	0.177	0.283	0.291
10	0.76	0.77	0.197	0.266	0.291

Table 5. Comparison of identification confidence, verification similarity, and image quality metrics across different numbers of guide images employed in MASQUE.

Guide Method	Iden. DSR( $\uparrow$ )	Veri. DSR( $\uparrow$ )	PSNR( $\uparrow$ )
Pairwise ( $G = 1$ )	0.72	0.66	25.691
Self-Guidance ( $G = 0$ )	0.56	0.40	25.812
+ Horizontal Flip	0.57	0.50	25.834
+ Vertical Flip	0.12	0.06	26.566
+ Translation	0.55	0.38	25.807

Table 6. Impact of adversarial image guidance in DSR and PSNR. We test pairwise- and self-guidance with different augmentations.

identity-relevant cues and inject subtle adversarial signals that steer the diffusion process away from a recognizable identity manifold. The guide image serves as a proxy for the gallery image, providing guidance on the direction in which the latent representation should be altered. This eliminates reliance on external identities, mitigating ethical concerns related to impersonation while ensuring identity protection remains non-intrusive.

Leveraging multiple guide images further stabilizes adversarial training, reducing bias toward any single representation and improving robustness. To evaluate its effectiveness, we use FaceNet as the target model and select 100 identities from CelebA-HQ, varying the number of guide images per identity. These evaluation identities are distinct from the main experiments, ensuring at least 12 images per identity to accommodate setups with up to 10 guide images.

Effectiveness is measured using the confidence score, the gap between the similarity score of the original identity’s gallery image and that of the misidentified identity. Table 5 shows that increasing guide images enhances identity obfuscation, leading to higher confidence scores while reducing similarity with the original identity. Moreover, images generated with guide images in the pairwise adversarial guidance step exhibit higher visual quality than those relying solely on adversarial loss on the original image. This confirms that simply maximizing distance from the original image is ineffective, as it disrupts the diffusion process’s goal of preserving natural image characteristics, leading to instability in both image quality and adversarial performance. These results demonstrate that MASQUE’s pairwise adversarial guidance provides a robust, privacy-centric solution, balancing strong identity obfuscation with high visual fidelity.

	AMT-GAN	DiffAM	C2P (I)	C2P (D)	MASQUE
Rank-1	54.39	61.25	36.92	71.17	92.08
Rank-5	28.58	45.58	18.25	48.67	81.42

Table 7. DSR with Rank-1 and Rank-5 metrics across AFR methods

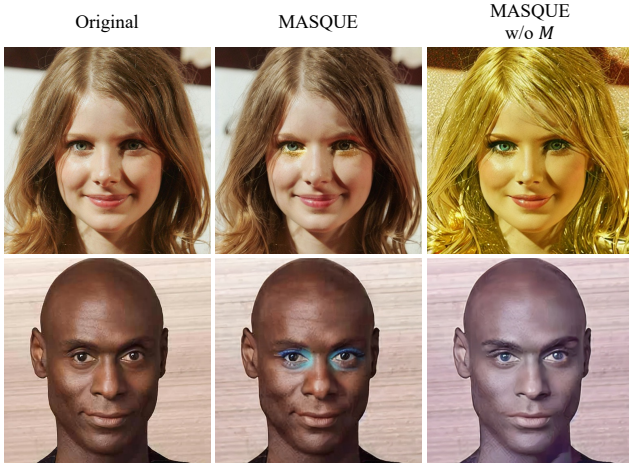


Figure 7. Visualizations of MASQUE with and without masking. The first row uses prompt “shimmery gold eyeshadow”, while the second row uses “blue eyeshadow”.

### B.3. Self-Augmented Guidance

To address cases where users may lack suitable guide images, we tested using self-augmented input images as guide images. This experiment was conducted on 100 identities from CelebA-HQ with the prompt “red lipstick”, targeting the FaceNet model. For augmentation, we applied horizontal flipping, vertical flipping, and random translation with a maximum shift of 20 pixels. Results, as shown in Table 6, compare these approaches against the input image itself as the guide image. Horizontal flipping and random translation perform similarly to using the input image as the guide, whereas vertical flipping shows minimal adversarial effect. This is likely because vertically flipped faces are hard to align with facial images by the recognition model.

### B.4. DSR under Rank-5 Accuracy

We also report DSR for the face identification task, using rank-5 accuracy to assess dodging success. The results are presented in Table 7. Notably, MASQUE achieves the highest DSR in both rank-1 and rank-5 settings, demonstrating its effectiveness in misleading identification models.

### B.5. Mask and Perturbation Localization

To understand the impact of masking in MASQUE, we conduct an ablation study with and without applying a mask. Figure 7 shows that the absence of a mask causes the model to struggle with spatial control, leading to unconstrained

perturbations across the entire image rather than confining makeup to the intended area.

## C. Additional Visualizations

Additional visual results of image-guided makeup transfer are provided in Figure 8 to accommodate space limitations in the main text. MASQUE demonstrates precise makeup application for each prompt, regardless of the targeted region or the subject’s demographics.

To evaluate color variation, we provide examples featuring both a male and a female subject. Additionally, by testing prompts that target different facial regions (eyes, lips, cheeks, skin, and full-face makeup), we demonstrate MASQUE’s ability to generate realistic makeup across various regions. We further provide visualizations without  $\mathcal{L}_{\text{edit}}$  optimization to illustrate its impact.



Figure 8. Visualizations of MASQUE-generated images with or without using the edit loss.

## D. Algorithm Pseudocode

---

### Algorithm 1 Adversarial Makeup Generation with CA Guidance

---

**Input:**  $z_{\text{edit}}, z_{\text{rec}}$ : Edited and original latent,  $e_{\text{edit}}, e_{\text{rec}}$ : Edited and original text embeddings,  $\mathcal{D}$ : Stable Diffusion model,  $T$ : Number of diffusion steps,  $\tau_{\text{attn}}, \tau_{\text{edit}}, \tau_{\text{adv}}$ : Step thresholds,  $\mathcal{M}$ : Binary region mask,  $\mathcal{I}_{\text{target}}$ : Target token indices,  $d_k$ : Key/Query dimensionality,  $\lambda_{\text{edit}}, \lambda_{\text{CoSi}}, \lambda_{\text{LPIPS}}$ : Loss weights,  $\eta$ : Learning rate,  $\sigma(t)$ : Noise scale function,  $x$ : Input image,  $\tilde{x}$ : Guide image,  $max\_adv$ : Maximum adversarial iterations

**Output:** Final protected image  $x_p$

```

for  $k \leftarrow T$  to 1 do
  if  $k > T - \tau_{\text{attn}}$  then
    //Perform cross-attention edit
     $CA^{\text{refined}} \leftarrow \{\}$ 
    for  $\ell \in \text{CrossAttnLayers}$  do
       $Q_\ell, K_\ell, V_\ell \leftarrow \mathcal{D}.\text{UNet}.\text{GetCrossAttentionComponents}(z_{\text{edit}}, e_{\text{edit}}, \ell)$ 
       $CA_\ell \leftarrow \text{Softmax}\left(\frac{Q_\ell K_\ell^\top}{\sqrt{d_k}}\right)$ 
       $CA_\ell^{\text{refined}} \leftarrow CA_\ell \cdot V_\ell$ 
       $CA^{\text{refined}} \leftarrow CA^{\text{refined}} \cup \{CA_\ell^{\text{refined}}\}$ 
  if  $k > T - \tau_{\text{edit}}$  then
    //Perform edit loss update
     $\mathcal{L}_{\text{edit}} \leftarrow 0$ 
    foreach  $CA_\ell^{\text{refined}} \in CA^{\text{refined}}$  do
       $CA_{\text{target}} \leftarrow \text{ExtractTargetAttention}(CA_\ell^{\text{refined}}, \mathcal{I}_{\text{target}})$ 
       $CA_{\text{masked}} \leftarrow CA_{\text{target}} \odot \mathcal{M}$ 
       $\mathcal{L}_{\text{edit}} \leftarrow \mathcal{L}_{\text{edit}} + \frac{(\sum_{(i,j) \in \mathcal{M}} CA_{\text{masked}}[i,j])^2}{\sum_{(i,j) \in \mathcal{M}} \mathcal{M}[i,j]}$ 
     $\mathcal{L}_{\text{edit}} \leftarrow \frac{\mathcal{L}_{\text{edit}}}{|CA^{\text{refined}}|}$ 
     $\nabla_{z_{\text{edit}}} \mathcal{L}_{\text{edit}} \leftarrow \text{Backprop}(\mathcal{L}_{\text{edit}})$ 
     $z_{\text{edit}} \leftarrow z_{\text{edit}} - \eta \cdot \lambda_{\text{edit}} \cdot \nabla_{z_{\text{edit}}} \mathcal{L}_{\text{edit}}$ 
  //Apply classifier-free guidance during all diffusion steps
   $\epsilon_{\text{rec}} \leftarrow \mathcal{D}.\text{UNet}(z_{\text{rec}}, t_k, e_{\text{rec}})$ 
   $\epsilon_{\text{edit}} \leftarrow \mathcal{D}.\text{UNet}(z_{\text{edit}}, t_k, e_{\text{edit}}, CA^{\text{refined}})$ 
   $z_{\text{rec}} \leftarrow z_{\text{rec}} - \sigma(t_k) \cdot \epsilon_{\text{rec}}$ 
   $z_{\text{edit}} \leftarrow z_{\text{edit}} - \sigma(t_k) \cdot \epsilon_{\text{edit}}$ 
   $z_{\text{edit}} = \mathcal{M} \cdot z_{\text{edit}} + (1 - \mathcal{M}) \cdot z_{\text{rec}}$ 
  if  $k < T - \tau_{\text{adv}}$  then
    //Perform pairwise adversarial optimization
    for  $i \leftarrow 0$  to  $max\_adv - 1$  do
       $x_{\text{rec}} \leftarrow \mathcal{D}.\text{VAE}.\text{Decode}(z_{\text{edit}})$ 
       $\mathcal{L}_{\text{adv}} \leftarrow \lambda_{\text{CoSi}} \cdot \text{CoSi}(\text{FR}(x_{\text{rec}}), \text{FR}(\tilde{x})) + \lambda_{\text{LPIPS}} \cdot \text{LPIPS}(x_{\text{rec}}, x)$ 
       $grad \leftarrow \text{Backprop}(\mathcal{L}_{\text{adv}})$ 
       $z_{\text{edit}} \leftarrow z_{\text{edit}} - \eta \cdot grad$ 
       $z_{\text{edit}} \leftarrow z_{\text{edit}} \odot \mathcal{M} + z_{\text{rec}} \odot (1 - \mathcal{M})$ 
  //Decode the final latent to produce the protected image
   $x_p \leftarrow \mathcal{D}.\text{VAE}.\text{Decode}(z_{\text{edit}})$ 
return  $x_p$ 

```

---